Supporting information for the paper:

Understanding the Evolution of Luminescent Gold Quantum Clusters in Protein Templates

Kamalesh Chaudhari, [†,‡] *Paulrajpillai Lourdu Xavier,* [‡] *Thalappil Pradeep*[*,‡]

†Department of Biotechnology and ‡DST Unit of Nanoscience (DST UNS), Department of Chemistry, Indian Institute of Technology Madras,

Chennai 600 036, India

*Address correspondence to

pradeep@iitm.ac.in

Table of contents

Supporting information 1. Time dependent MALDI MS of NLf in the presence and absence of NaOH.

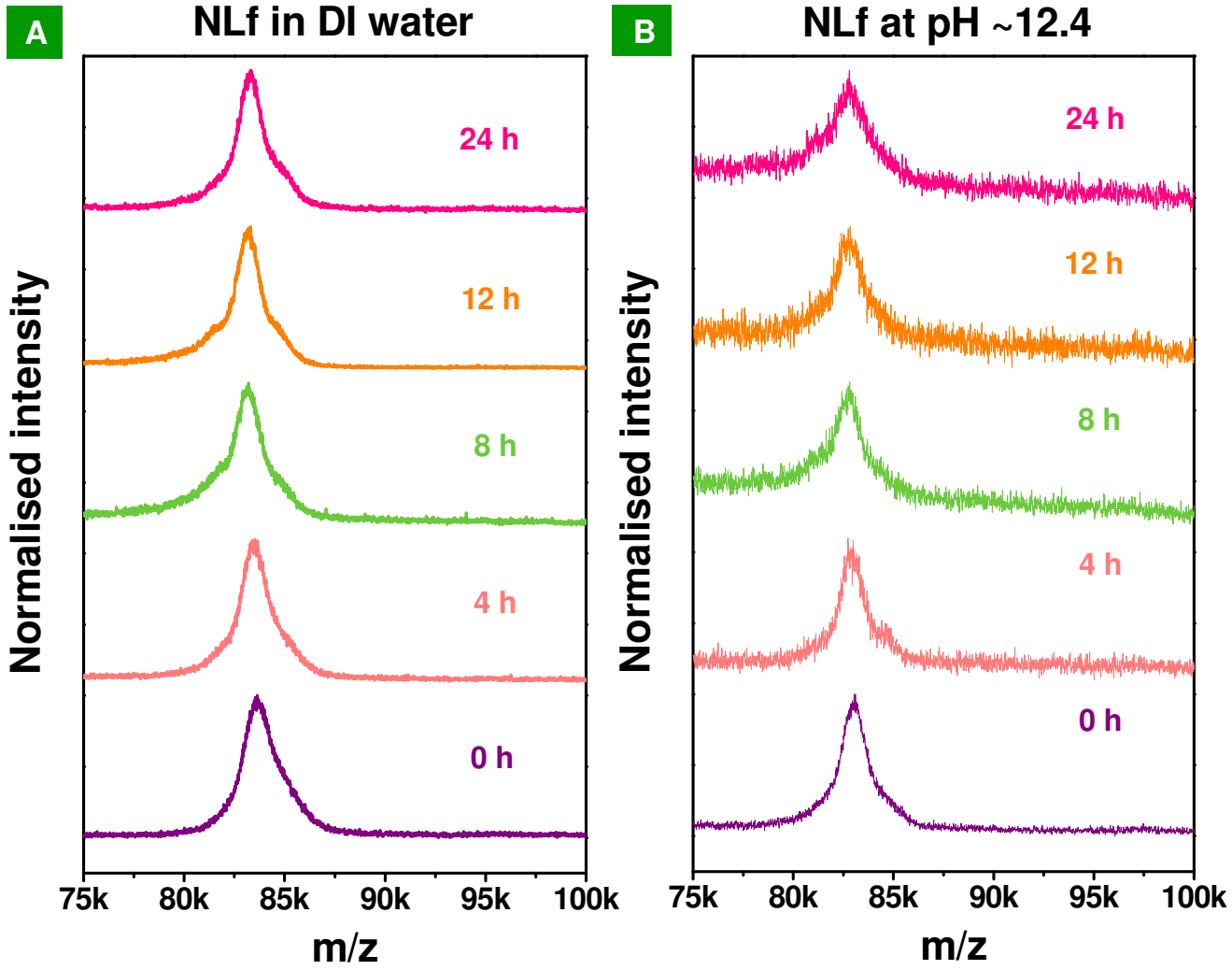

Figure S1. Time dependent MALDI MS data of (A) NLf in DI water (pH ~ 7) (average peak position ~ 83,338 Da) and (B) NLf at pH ~12.4 (average peak position ~ 82,842 Da). Peak difference is m/z 496, which proves that there is downshift in mass of NLf by ~500 at alkaline pH.

Experimental details to check reversibility of m/z value of NLf at basic pH

To check the reversibility of the downshift in mass caused by alkaline pH, we have performed an experiment in which MALDI MS of NLf samples at neutral pH and basic pH (5% NaOH) was monitored after 12 h. Then pH of NLf (in 5% NaOH) was reverted to neutral by adding HCl and MALDI MS analysis was done after 12 h. Averaging of 5 MS of all three samples have shown that downshift in mass of NLf is not reversible. Values obtained are as below,

NLf in DI water – m/z 83805

NLf at basic pH - m/z 83199

NLf at basic pH after reverting the pH – m/z 83112

Table 1. Change in percentage contribution of Au_{25}@NLf, Au_{13}@NLf and NLf with time. This relative quantification is obtained by peak fitting of the MALDI MS data.

% of NLf and Au_{QC}@NLf after 12 h of reaction			
Peak	Cluster	FWHM	Percentage contribution, %
1	Au_{25}@NLf	5670.775	88.82
2	Au_{13}@NLf	1773.100	4.04
3	NLf	1624.000	7.14
% of NLf and Au_{QC}@NLf after 72 h of reaction			
Peak	Cluster	FWHM	Percentage contribution, %
1	Au_{25}@NLf	5130.995	45.26
2	Au_{13}@NLf	3508.015	7.12
3	NLf	2903.470	47.61
% of NLf and Au_{QC}@NLf (after 48 h) when extra Au^{3+} was added to the parent reaction after 24 h			
Peak	Cluster	FWHM	Percentage contribution, %
1	Au_{25}@NLf	6643.915	79.80
2	Au_{13}@NLf	3517.271	---
3	NLf	3506.934	20.19

Supporting information 2. Photograph of Au_{QC}@NLf in visible and UV light at different times.

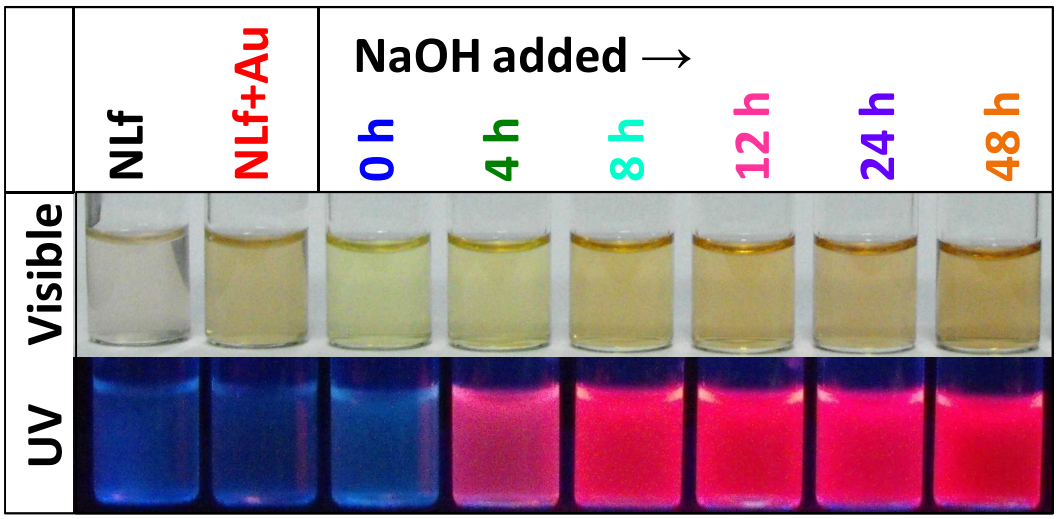

Figure S2. Photograph taken in visible and UV light to show the enhancement in luminescence intensity as a function of time in Au_{QC}@NLf system indicating the evolution of clusters.

Supporting information 3. Concentration dependent time evolution of the excitation spectra of Au_{QC}@NLf.

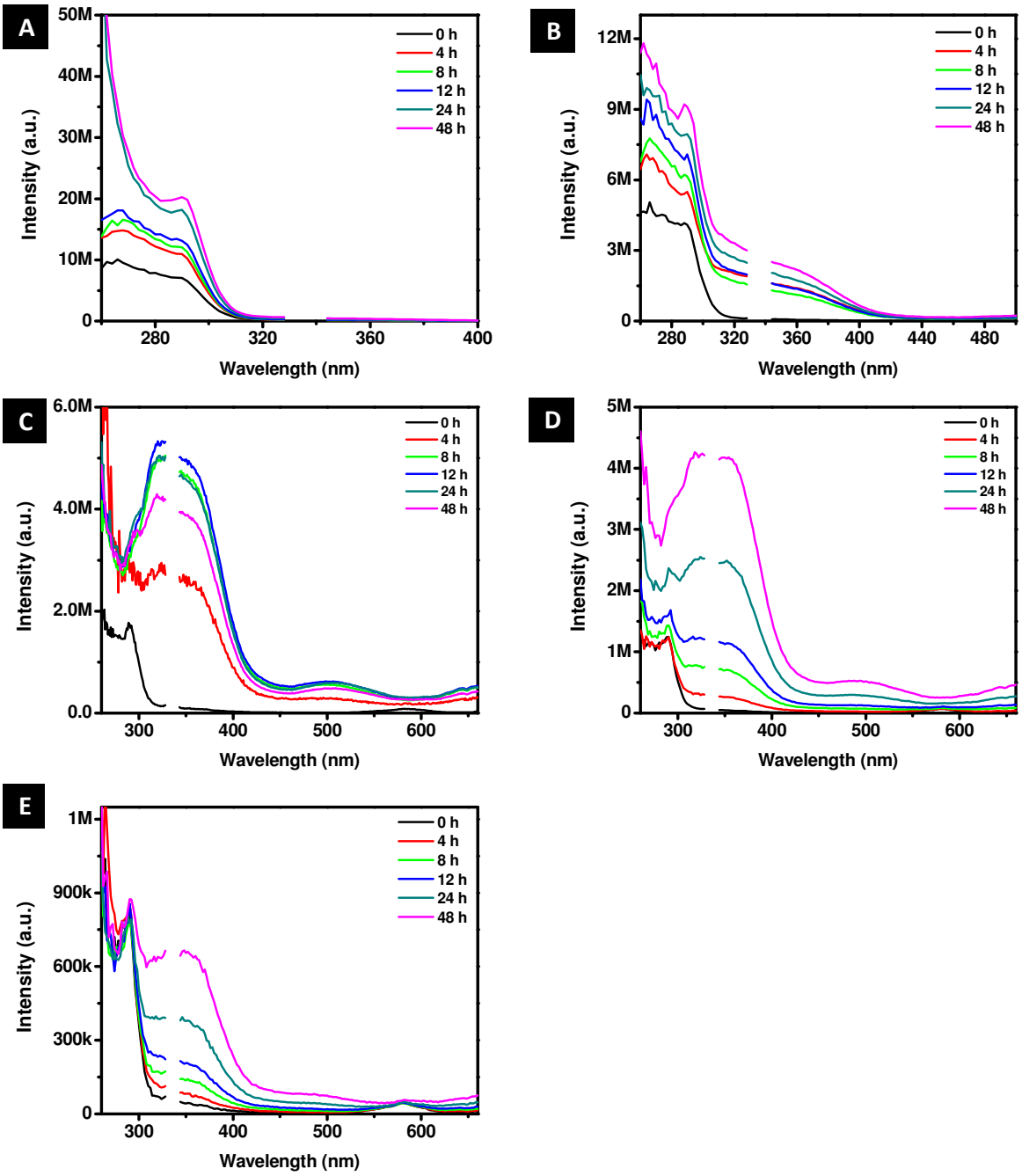

Figure S3. Incubation time dependent excitation spectra collected for the emission wavelength of 670 nm, indicating the evolution of cluster upon the interaction of Au^{3+} with NLf. NLf concentration was kept constant 150 µM while Au^{3+} concentration was varied as follows: (A) 0.5 mM, (B) 1.5 mM., (C) 2.5 mM, (D) 3.5 mM, and (E) 4.5 mM. Secondary peak at 335 nm is removed in these spectra.

Supporting information 4. Concentration dependent time evolution of the emission spectra of Au_{QC}@NLf.

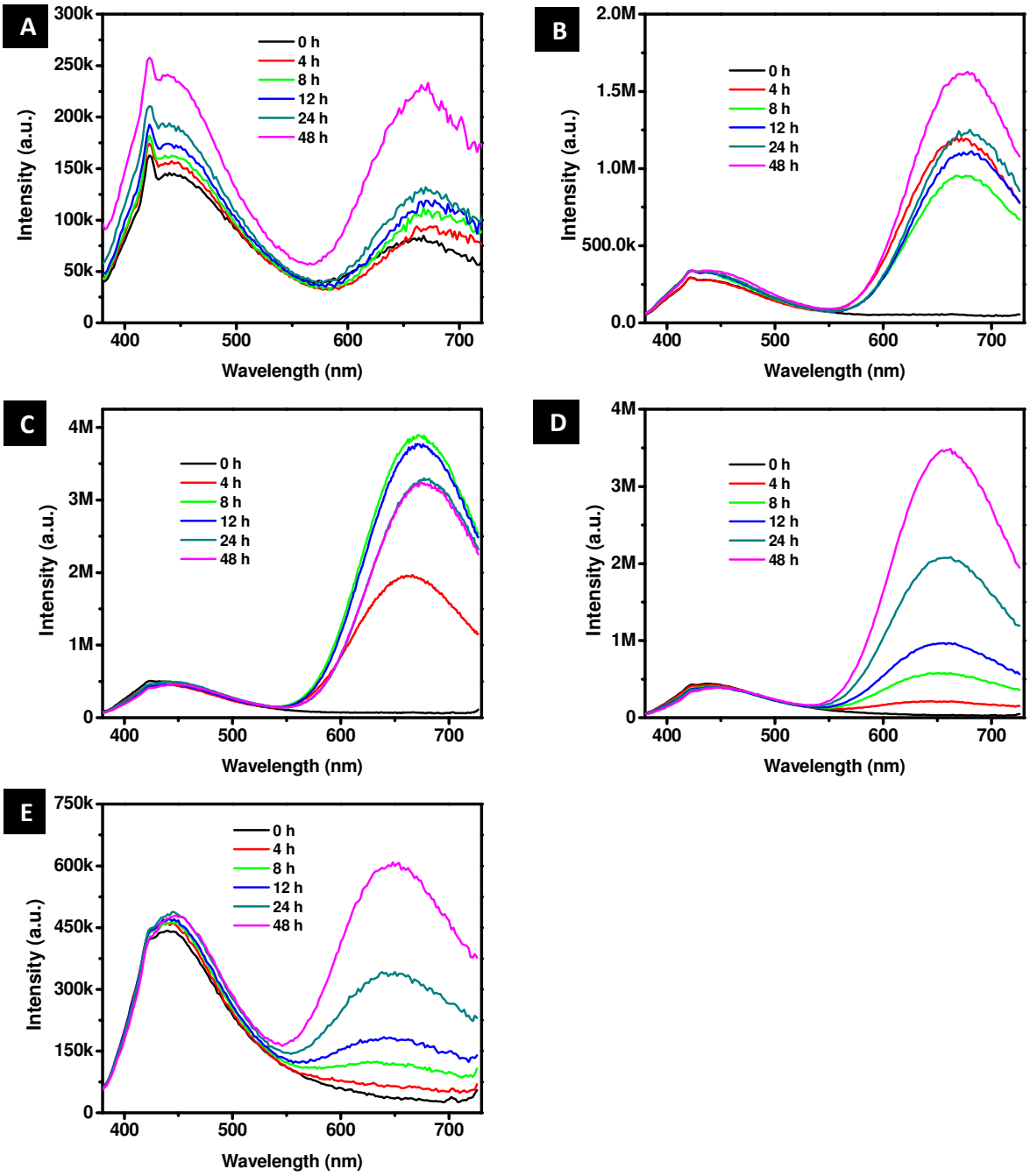

Figure S4. Time dependent emission spectra collected indicating evolution of the cluster as a function of incubation time of Au^{3+} with NLf in alkaline pH. NLf concentration was kept constant (150 µM) and Au^{3+} concentration was varied as (A) 0.5 mM, (B) 1.5 mM., (C) 2.5 mM, (D) 3.5 mM, and (E) 4.5 mM. Samples were excited at 370 nm.

Supporting information 5. Comparison between MALDI MS of Au_{QC}@NLf and Au_{QC}@$(NLf)_2$.

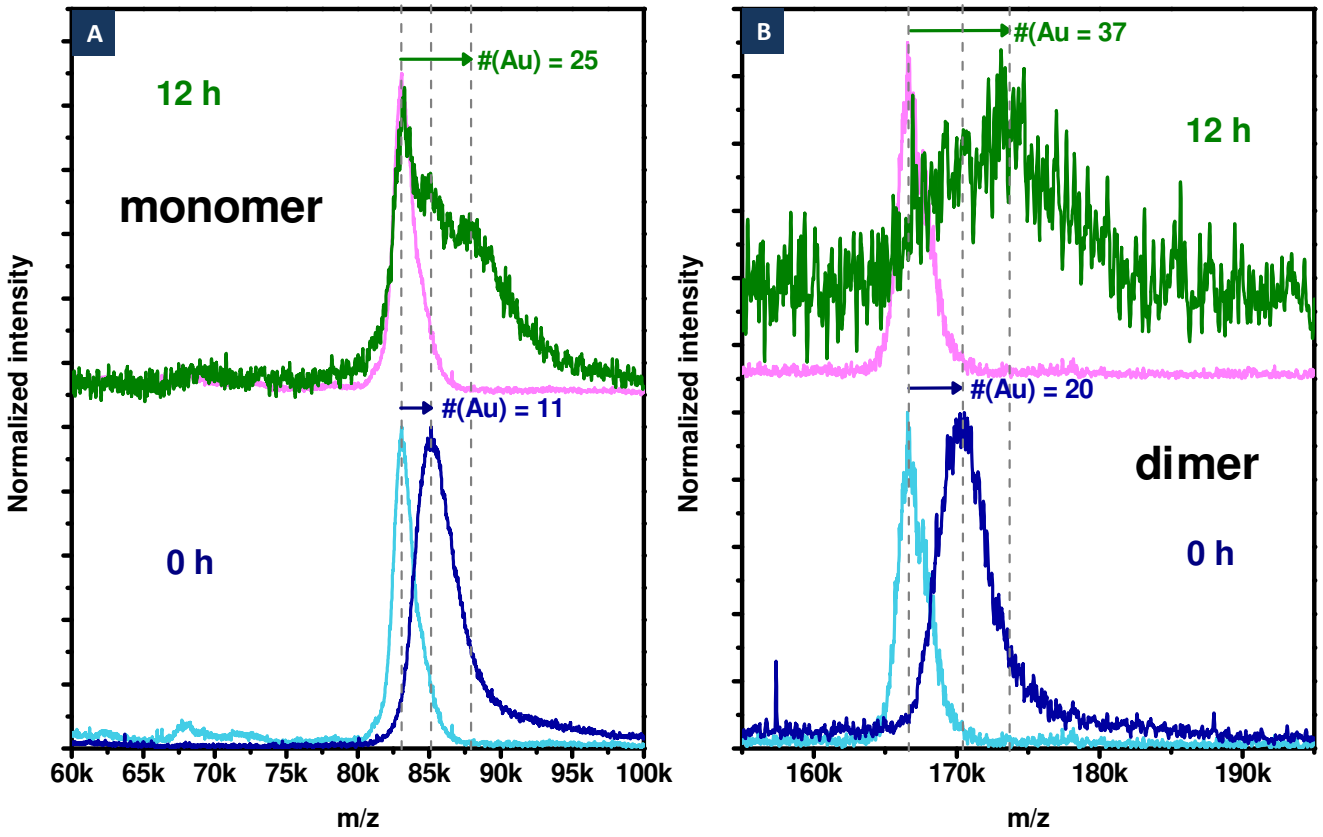

Figure S5. MALDI MS of (A) Au_{QC}@NLf and (B) Au_{QC}@$(NLf)_2$ at 0 and 12 h. The number of Au atoms added in the monomer and the dimer are shown with vertical lines. Note that in both the cases, the same mass window is shown.

Supporting information 6. Time evolution of the MALDI MS of Au_{QC}@NLf after 3 days.

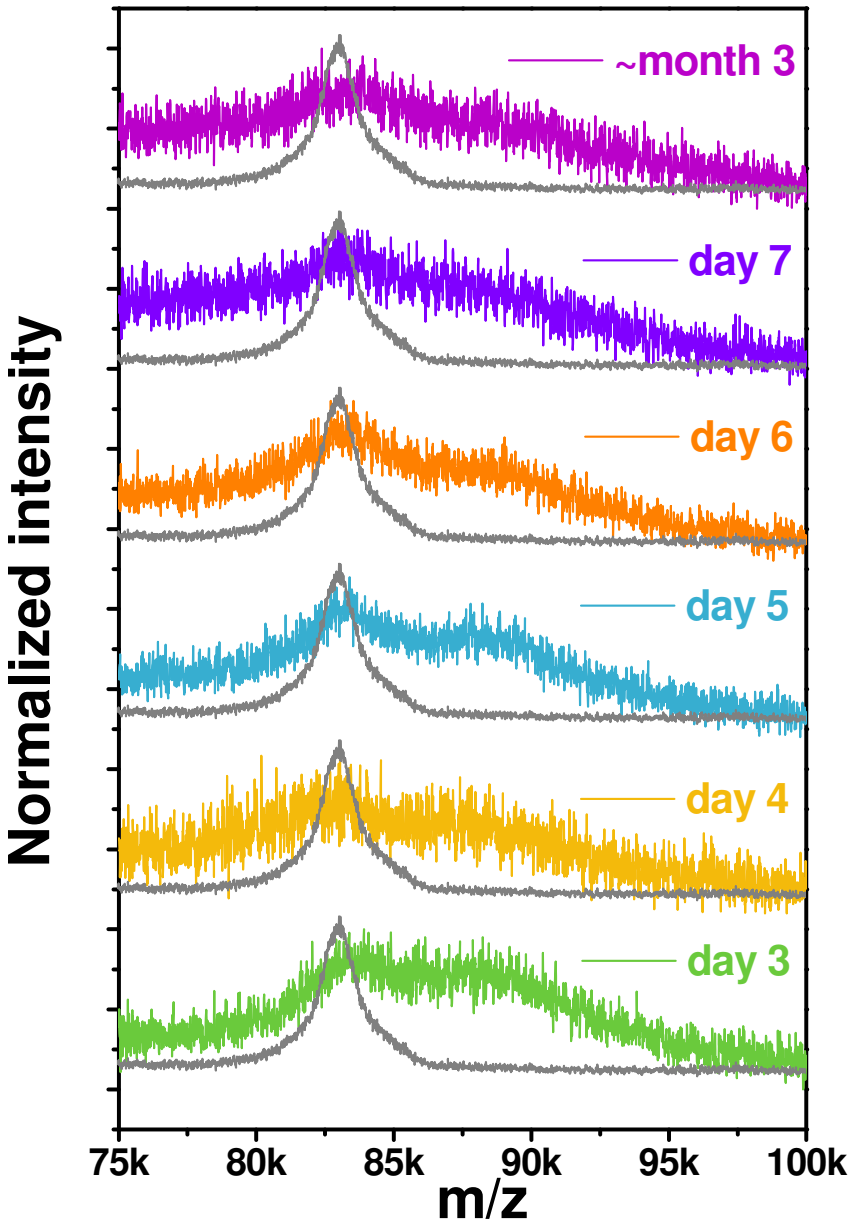

Figure S6. No considerable change was observed after 2 days when mass spectra were monitored for Au_{QC}@NLf (17:1 molar ratio of Au^{3+}:NLf). Reaction was carried out at alkaline pH (5% NaOH).

Supporting information 7. Saturation effect at 0 h for varying molar ratios of Au^{3+}:NLf.

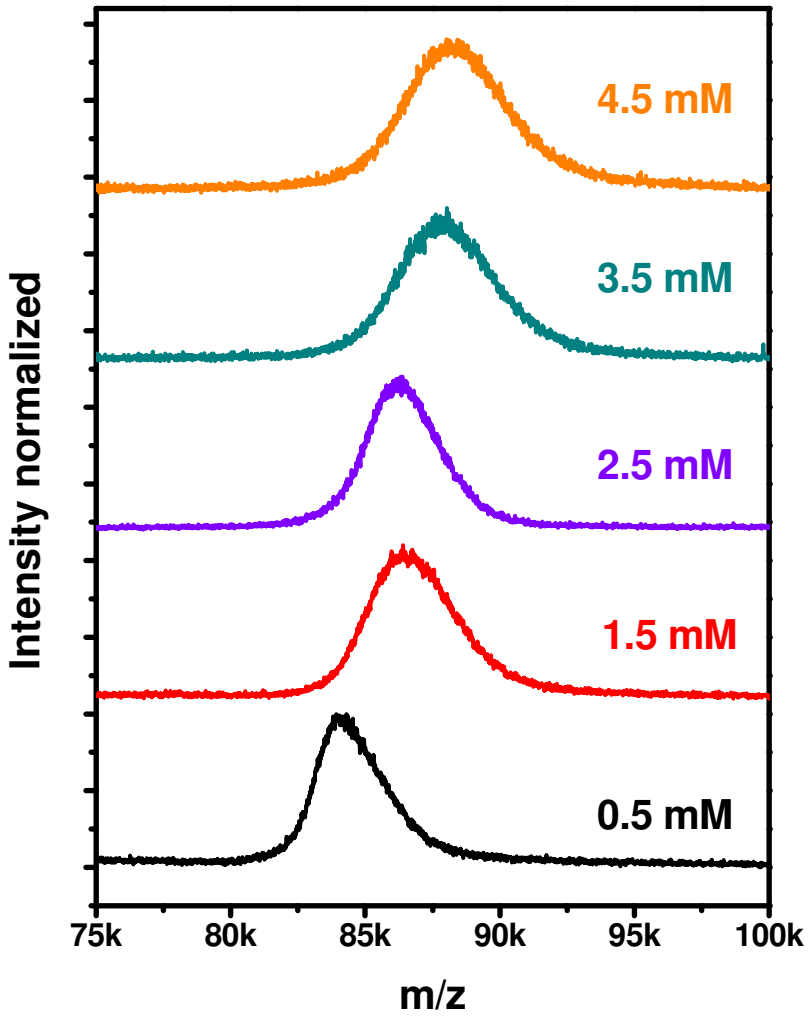

Figure S7. MALDI MS data showing saturation effect at 0 h when varying concentrations of Au^{3+} were added to the NLf solution (150 µM).

Supporting information 8. Luminescence spectrum of Au^{3+} and NLf mixture in the absence of NaOH.

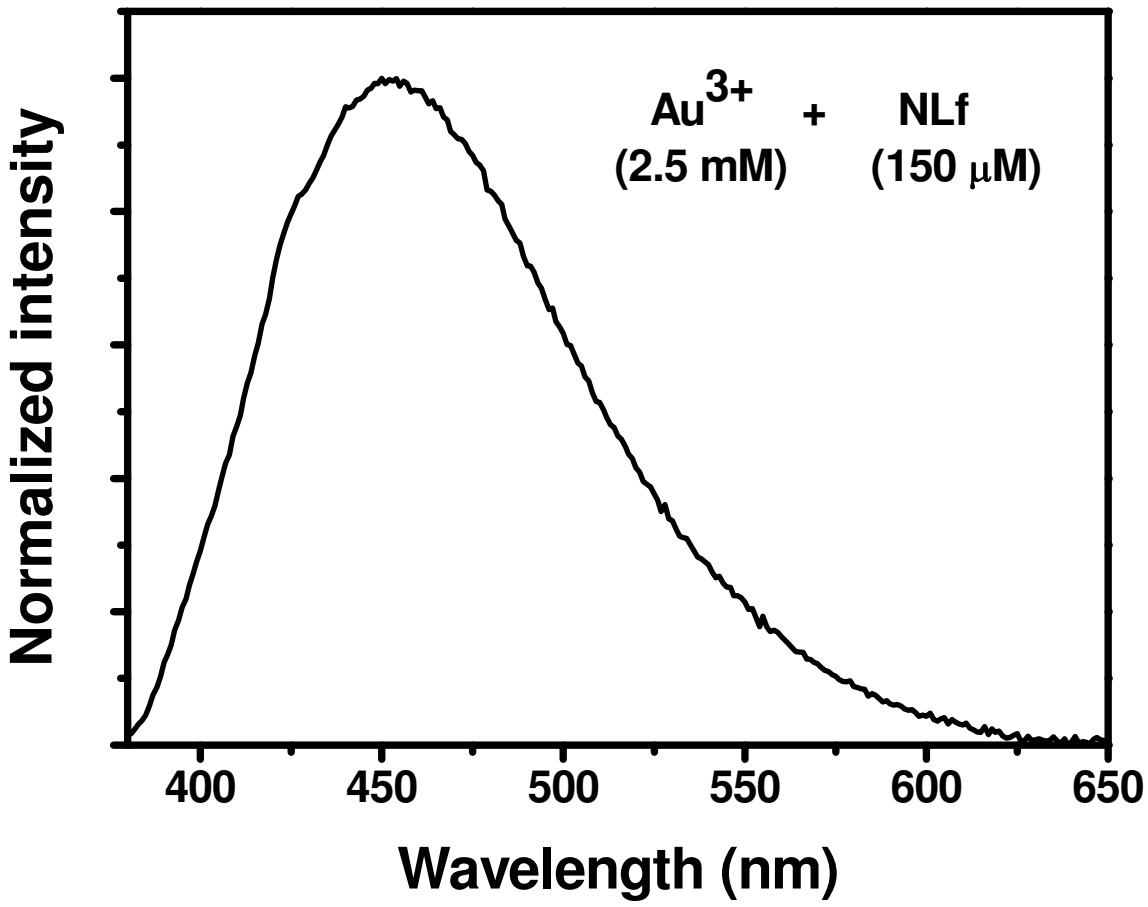

Figure S8. Luminescence spectrum of the reaction product when cluster synthesis was carried out in the absence of NaOH (pH ~ 7). Au^{3+}:NLf molar ratio was 17:1. In this case, only emission from the protein was seen.

Supporting information 9. Time evolution of the MALDI MS of Au_{QC}@NLf in the absence of NaOH.

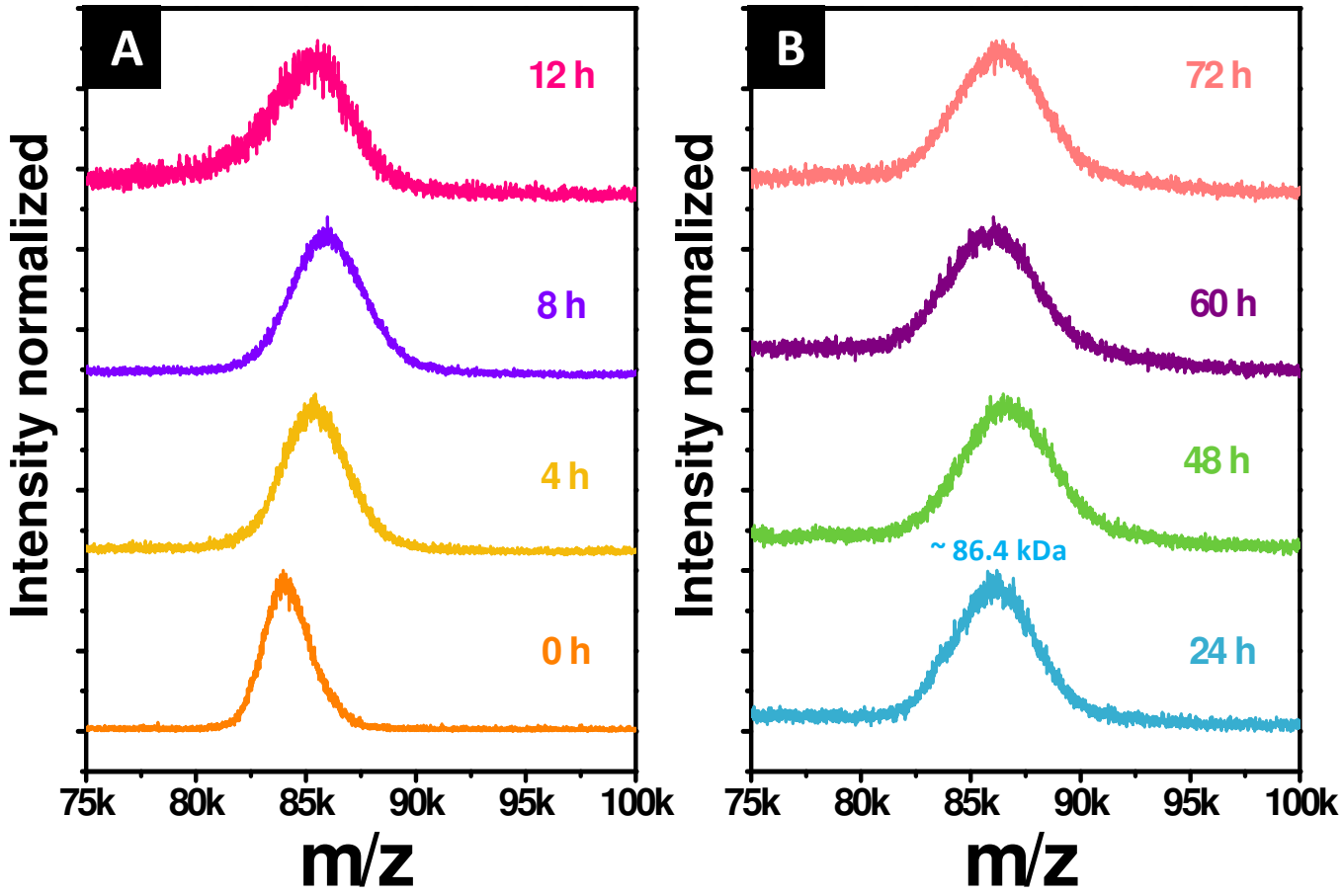

Figure S9. Mass spectra slight shift in mass of protein indicating the binding of Au^{3+} ions as a function of incubation time of Au^{3+} with NLf in the absence of NaOH. In the absence of alkaline pH, protein was observed to bind to 13- 14 Au ions and form Au^{+} - protein complex (see XPS data in Figure 5).

Supporting information 10. XPS of the S 2p region.

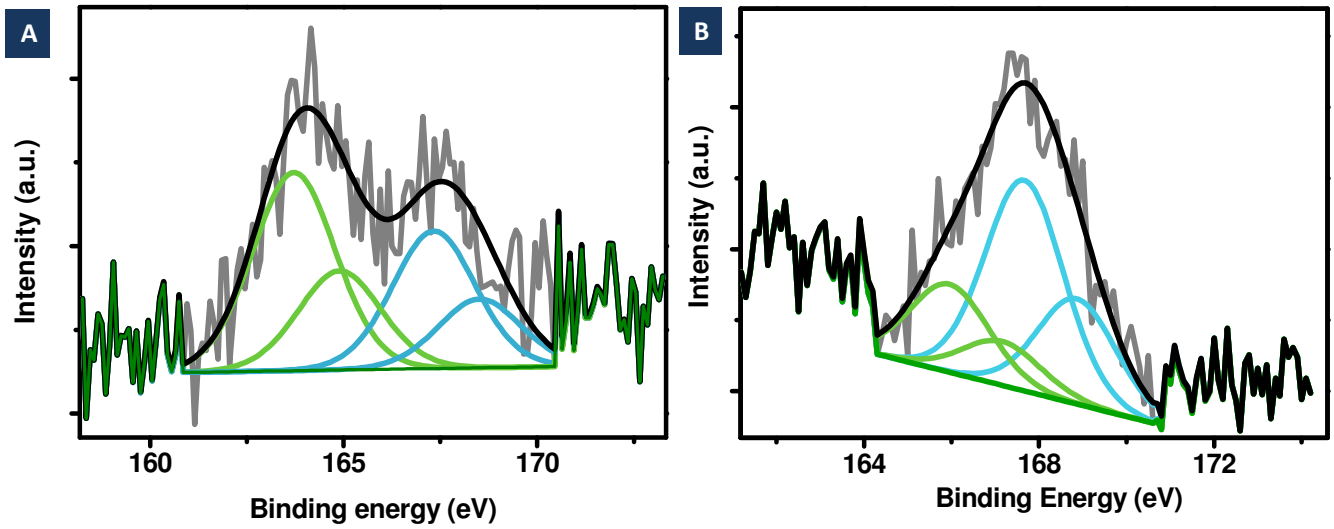

Figure S10. XPS of S 2p (A) before addition of NaOH and (B) 24 h after addition of NaOH. The region shows higher binding energy peaks due to sulfate, sulfite and sulfonate species as a result of X-ray beam induced damage.

Supporting information 11. Change in the emission peak position with time for different molar ratios of Au^{3+}:NLf.

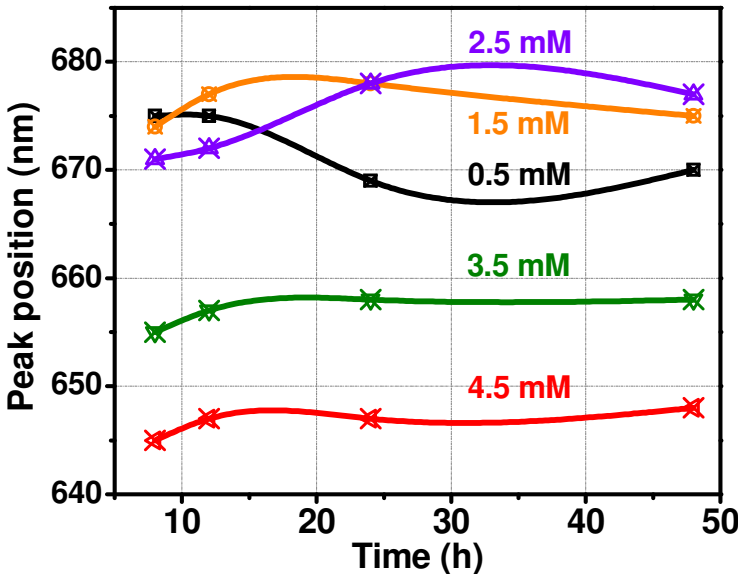

Figure S11. Emission peak positions for different Au^{3+} concentrations by keeping NLf concentration constant (150 µM) plotted against time, peak position shows blue shift with increasing concentration of Au^{3+} against NLf

Supporting information 12. Change in the emission peak position with time when pH of the sample was maintained constant.

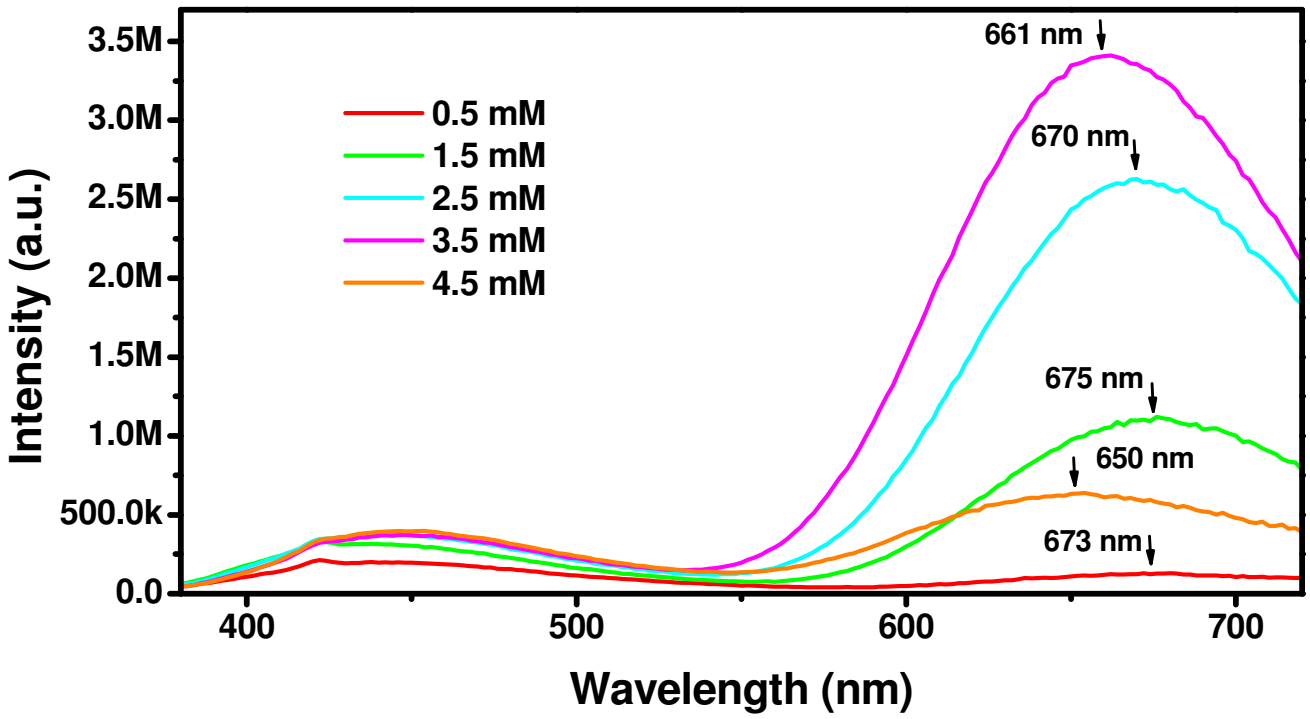

Figure S12. PL spectra of Au_{QC}@NLf with different Au^{3+}:NLf ratios. NLf concentration was kept constant (150 μM) and Au^{3+} concentration was varied from 0.5 mM-4.5 mM. The pH of the solution was kept constant at 12.4±0.03.

Supporting information 13. MALDI MS of Au_{QC}@NLf with time for different molar combinations of Au^{3+}:NLf at constant pH.

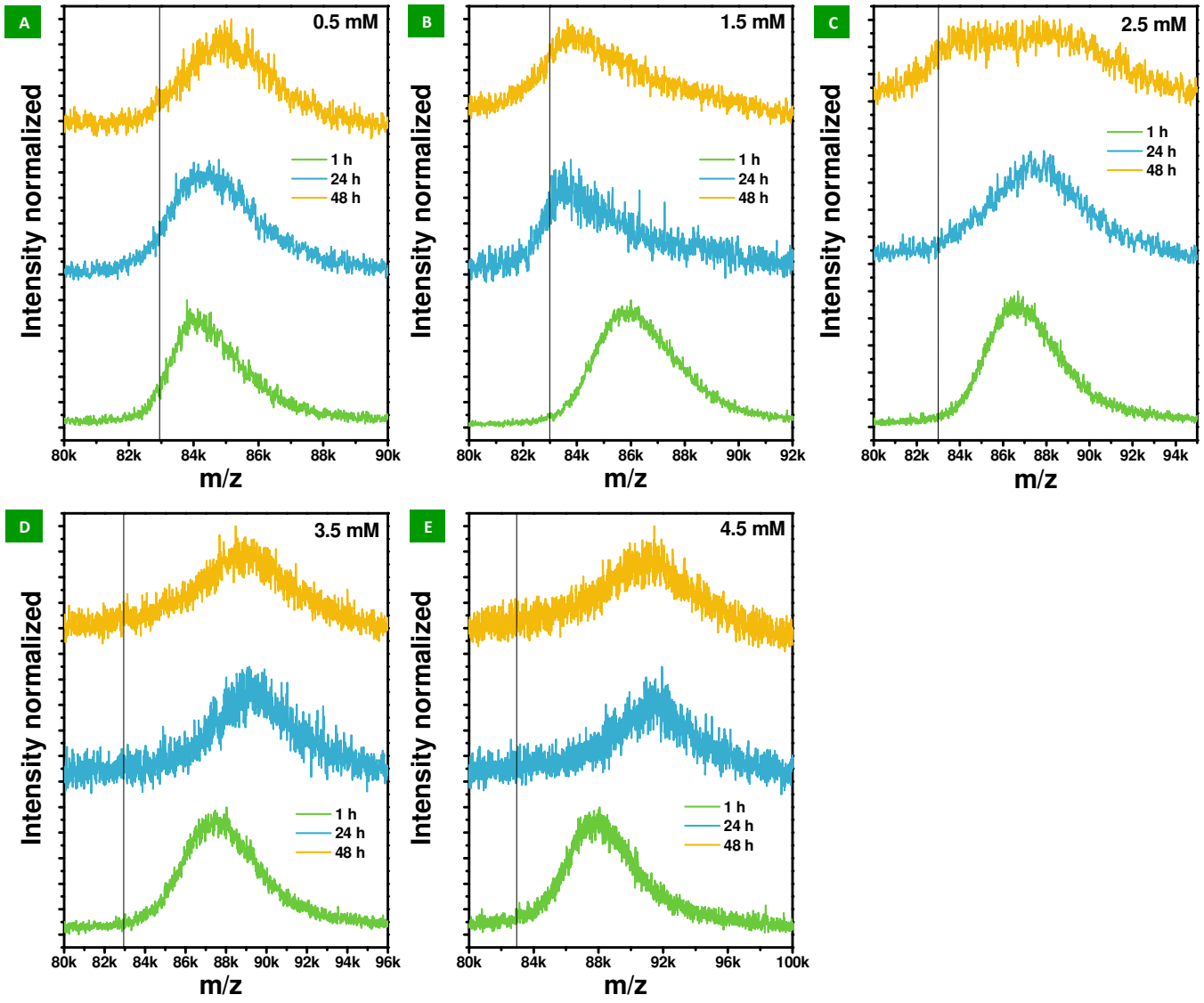

Figure S13. MALDI MS data of Au_{QC}@NLf as time progresses for varying Au^{3+}:NLf ratios. NLf concentration was kept constant (150 µM) and Au^{3+} concentration was varied as (A) 0.5 mM, (B) 1.5 mM, (C) 2.5 mM, (D) 3.5 mM, and (E) 4.5 mM. The pH of the solution was kept constant at 12.4±0.03. No noticeable change was observed in these mass spectra as compared to pH maintained samples. The occurrence of free protein is seen only at 48 h.

Supporting information 14. MALDI MS of the clusters synthesized by one step approach.

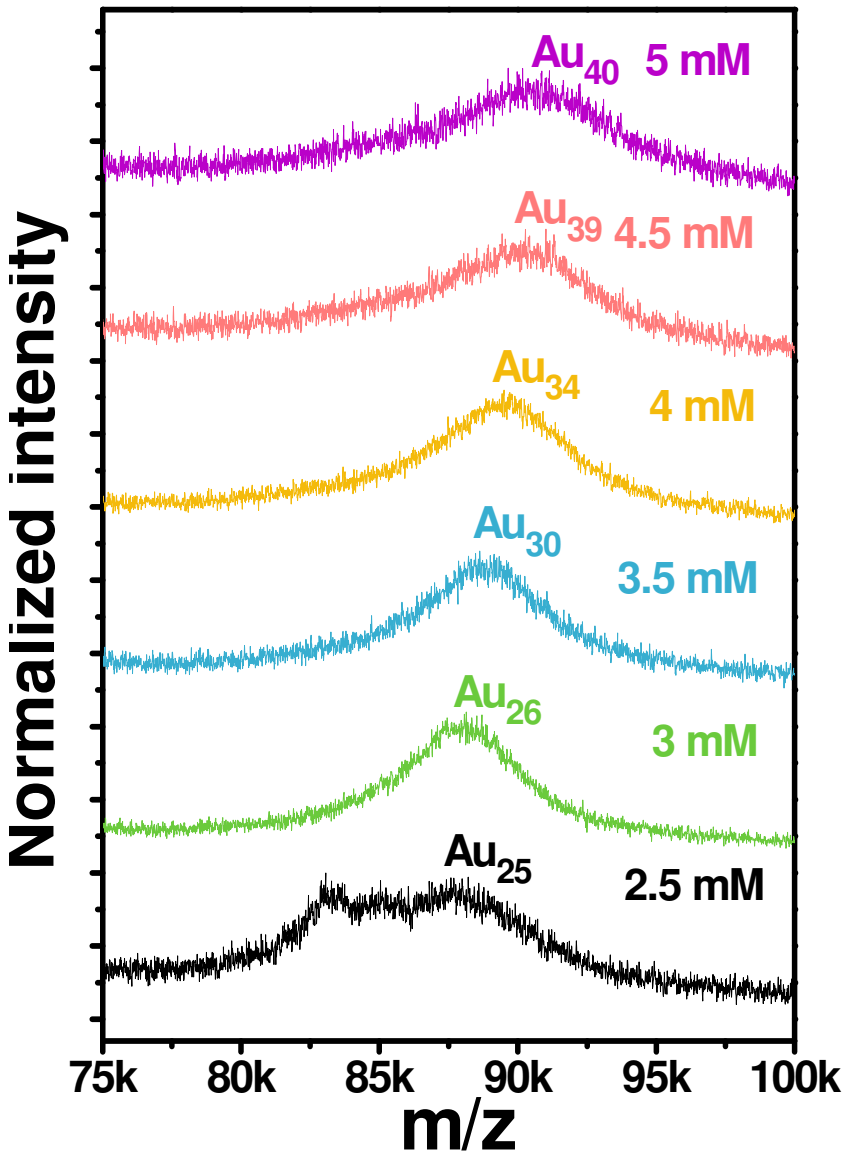

Figure S14. MALDI MS data of the clusters synthesized by one step approach. Spectra were collected after 48 h of reaction. Bigger sized clusters were seen upon addition of Au^{3+} above a concentration of 2.5 mM in the beginning of the reaction.

Supporting information 15. Photograph of the clusters synthesized by one step approach.

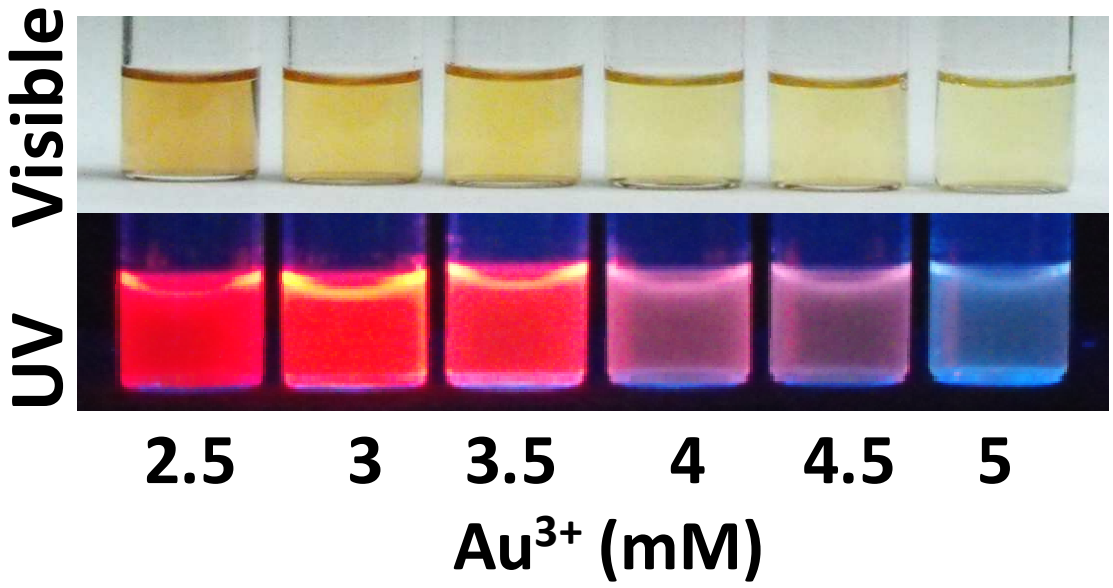

Figure S15. Photograph of the clusters synthesized by one step approach taken in the visible and UV light to show variations in the luminescence intensity of Au_{QC}@NLf by one step approach.

Supporting information 16. Time dependent UV-Vis spectra for different molar combinations of Au^{3+}:NLf.

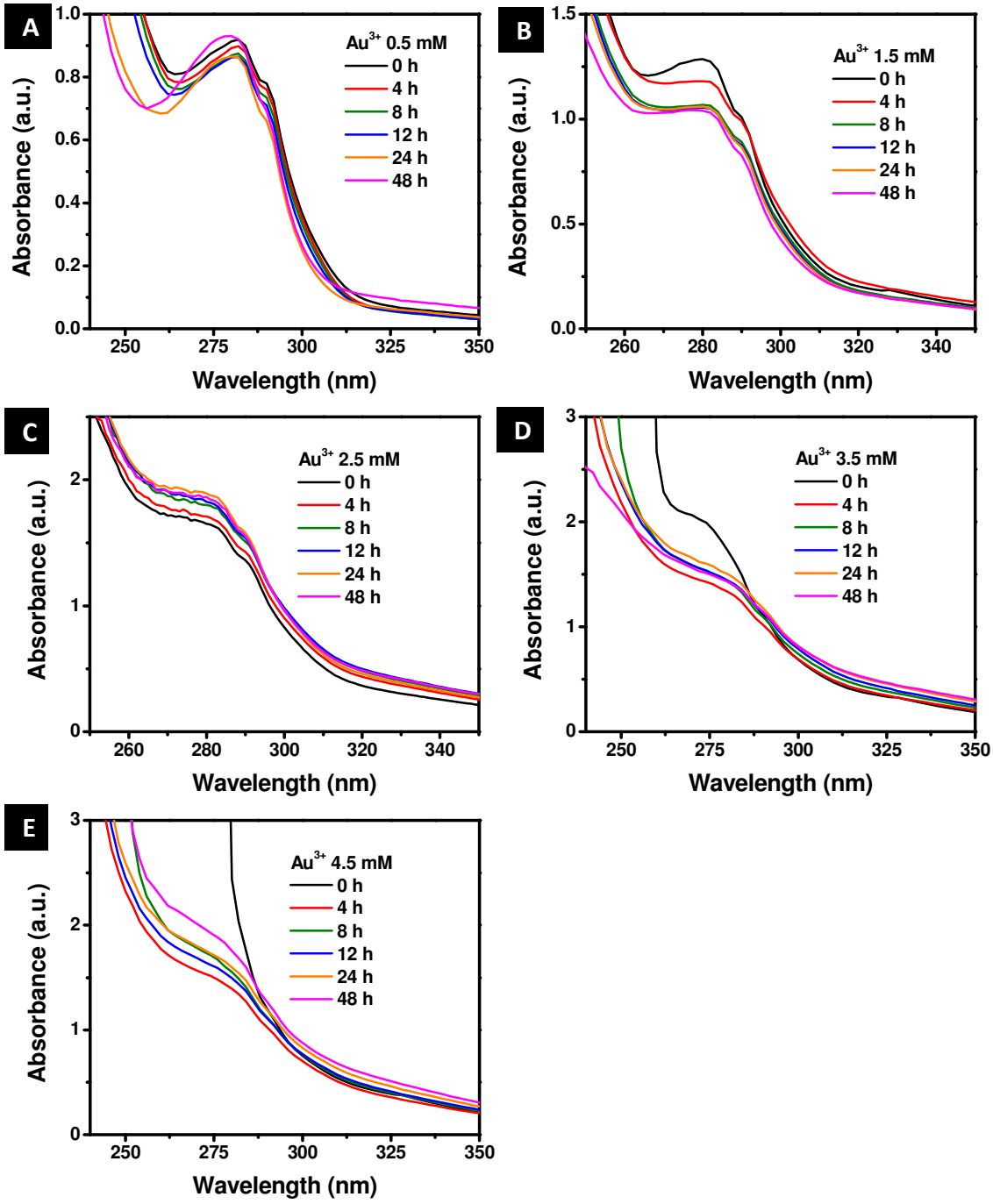

Figure S16. Time dependent UV-Vis spectra upon interaction of Au^{3+} with NLf. NLf concentration was kept constant (150uM) and Au^{3+} concentration was varied as (A) 0.5 mM, (B) 1.5 mM, (C) 2.5 mM, (D) 3.5 mM, and (E) 4.5 mM.

Supporting information 17. Time dependent UV-Vis spectra for different molar combinations of Au^{3+}:NLf.

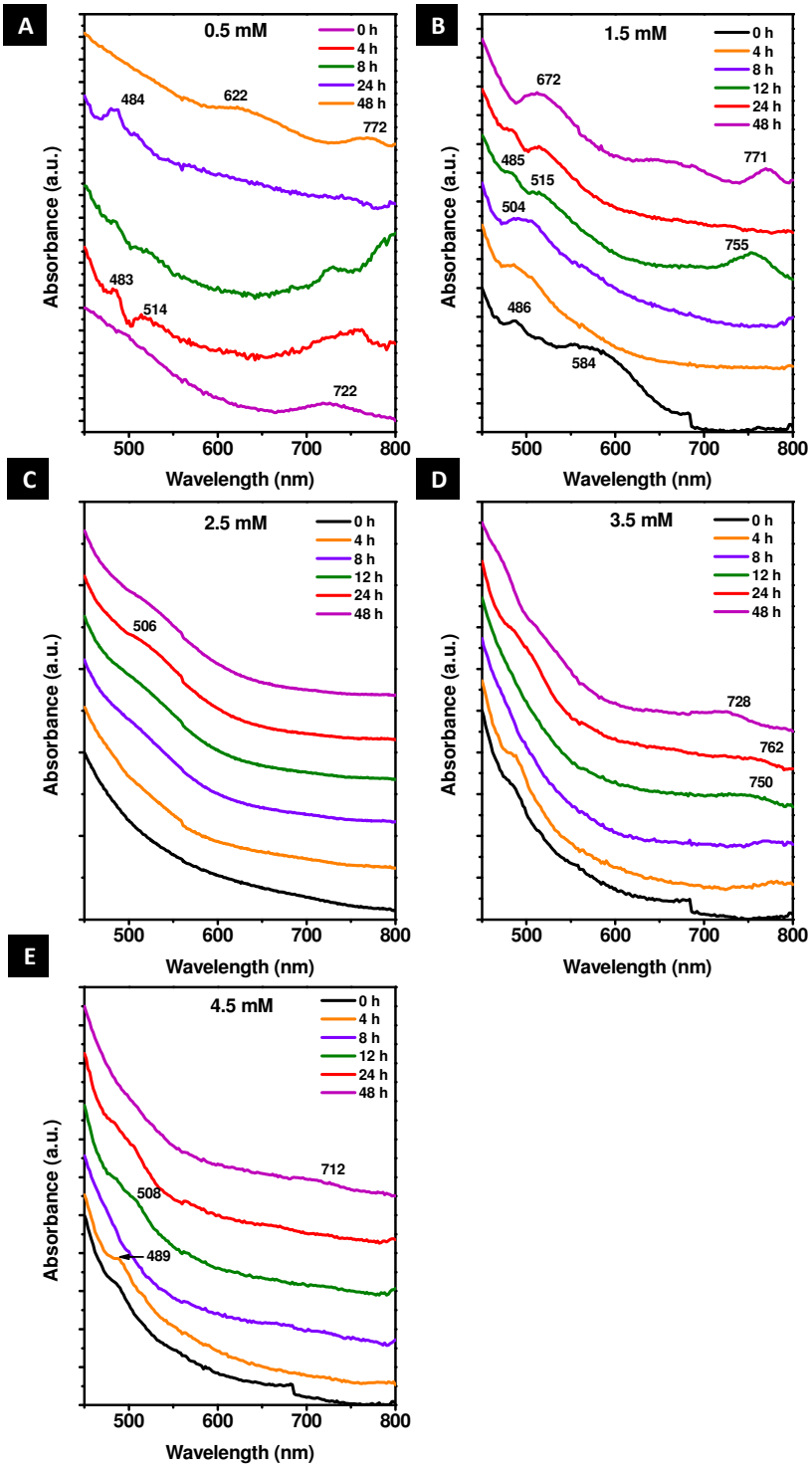

Figure S17. Time dependent UV-Vis spectra upon interaction of Au^{3+} with NLf; showing multiple features which are changing with time. NLf concentration was kept constant (150 µM) and Au^{3+} concentration was varied as (A) 0.5 mM, (B) 1.5 mM, (C) 2.5 mM, (D) 3.5 mM, and (E) 4.5 mM.

Scheme 1. Schematic for the synthesis of Au_{QC}@NLf by three different approaches.

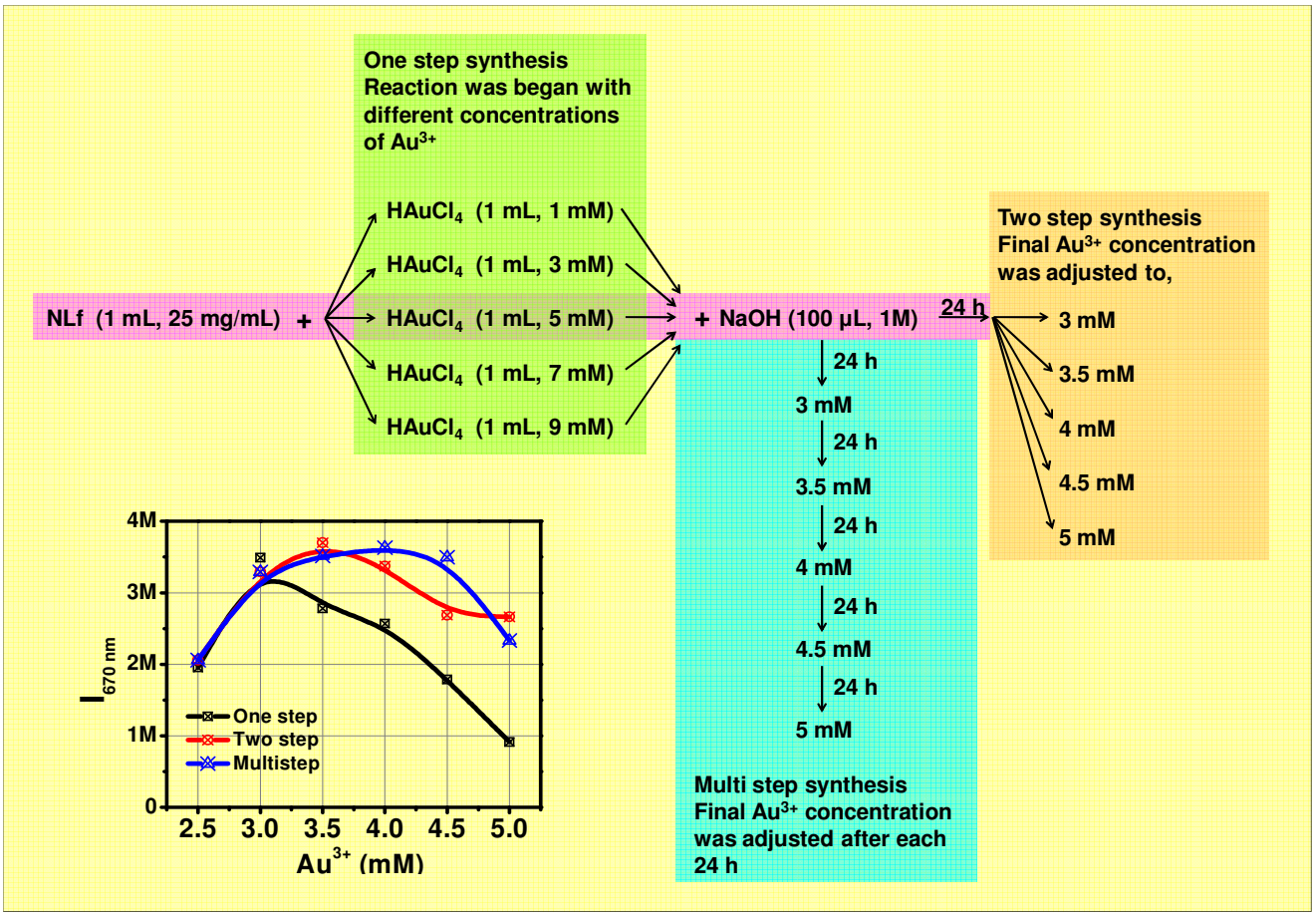

Scheme 1. Schematic showing different approaches used for attaining monodispersed clusters with enhanced luminescence.

Supporting information 18. MALDI MS and PL data of Au_{QC}@NLf synthesized by two step approach.

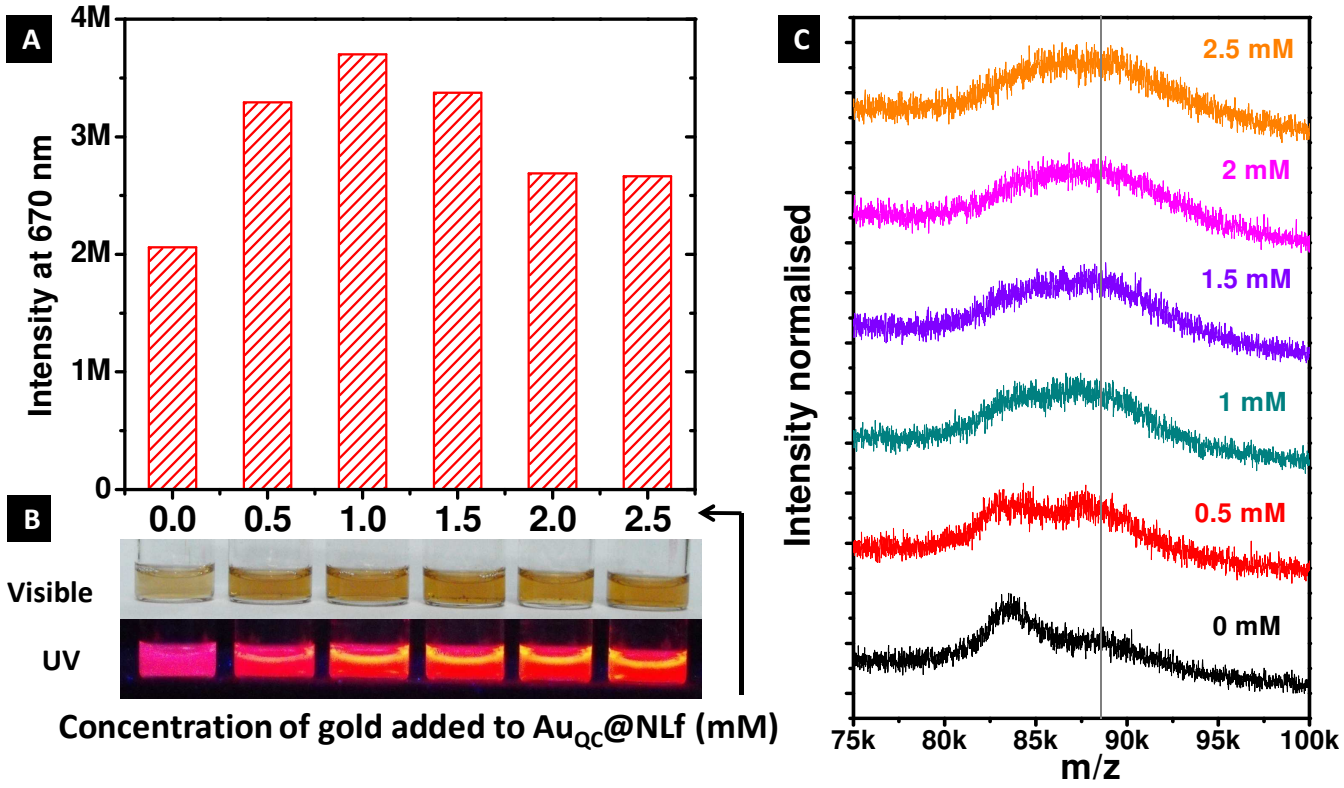

Figure S18. Au_{QC}@NLf were synthesized with the 17:1 molar ratio of Au^{3+}:NLf and after 24 h of reaction final concentration of Au^{3+} was adjusted from 3-5 mM to interact with the emerged free proteins (lost gold ions and became free during the reaction). (A) Bar diagram shows that 1 mM Au^{3+} is enough to consume the free protein and form additional clusters to enhance luminescence. (B) Photograph taken in visible and UV light to show enhanced luminescence. (C) MALDI MS shows relative reduction in the free NLf peak after addition of Au^{3+} and cluster growth.

Supporting information 19. UV-Vis spectra of Au_{QC}@NLf synthesized by three different approaches.

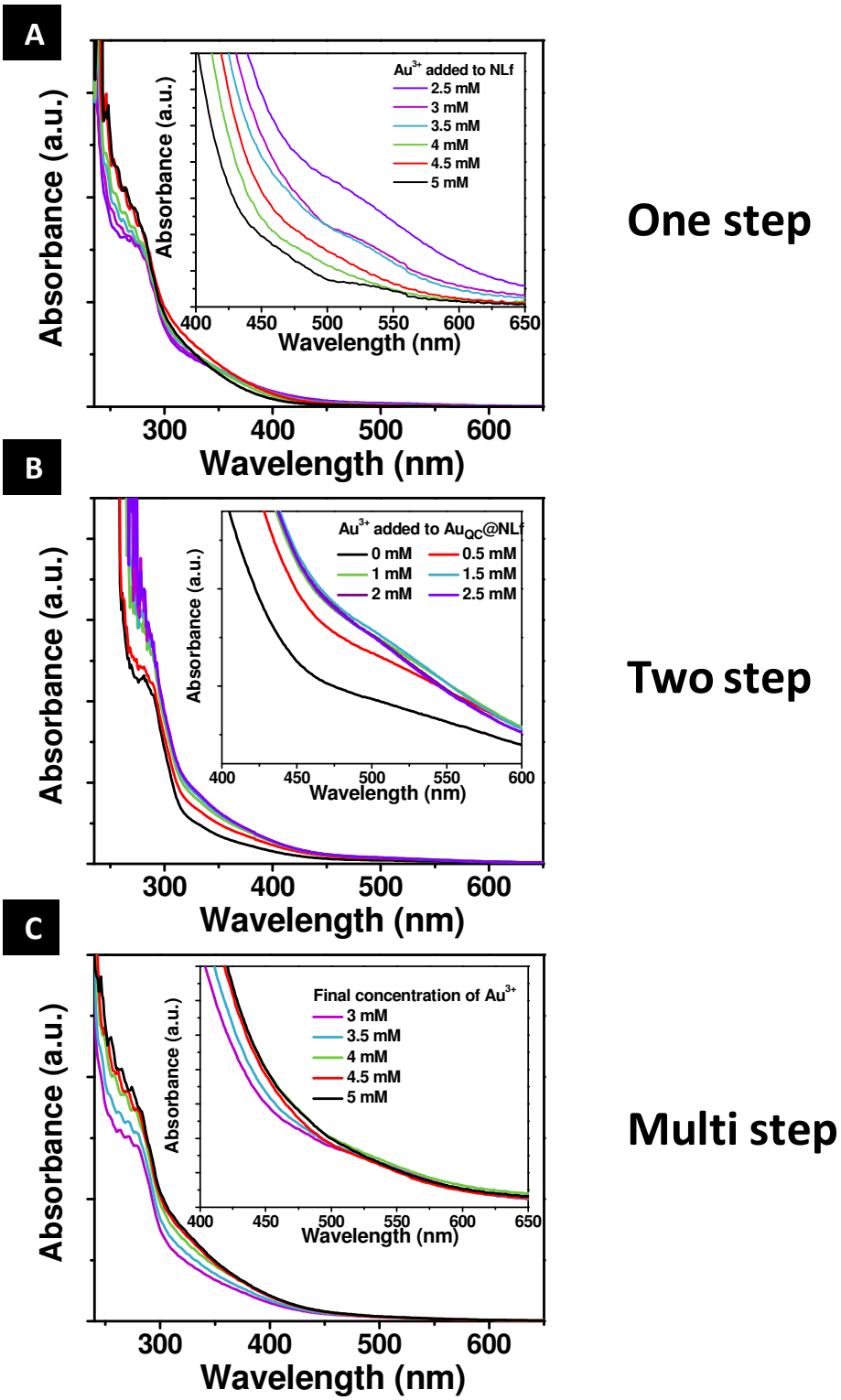

Figure S19. UV-Vis spectra of Au_{QC}@NLf measured after 48 h for three different approaches, (A) one step, (B) two step and (C) multi step.

Supporting information 20. MALDI MS data of the clusters synthesized with multistep approach.

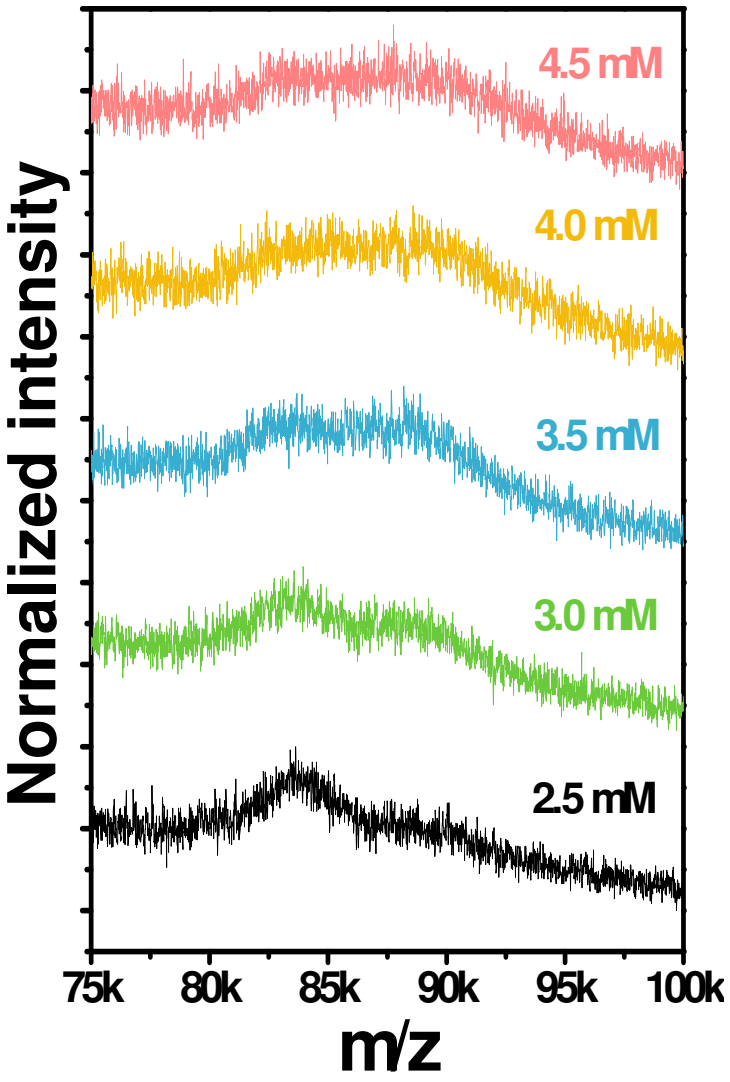

Figure S20. MALDI MS data of the clusters synthesized with multistep approach.

Supporting information 21. UV-Vis spectra of Au_{QC}@BSA at various stages of evolution.

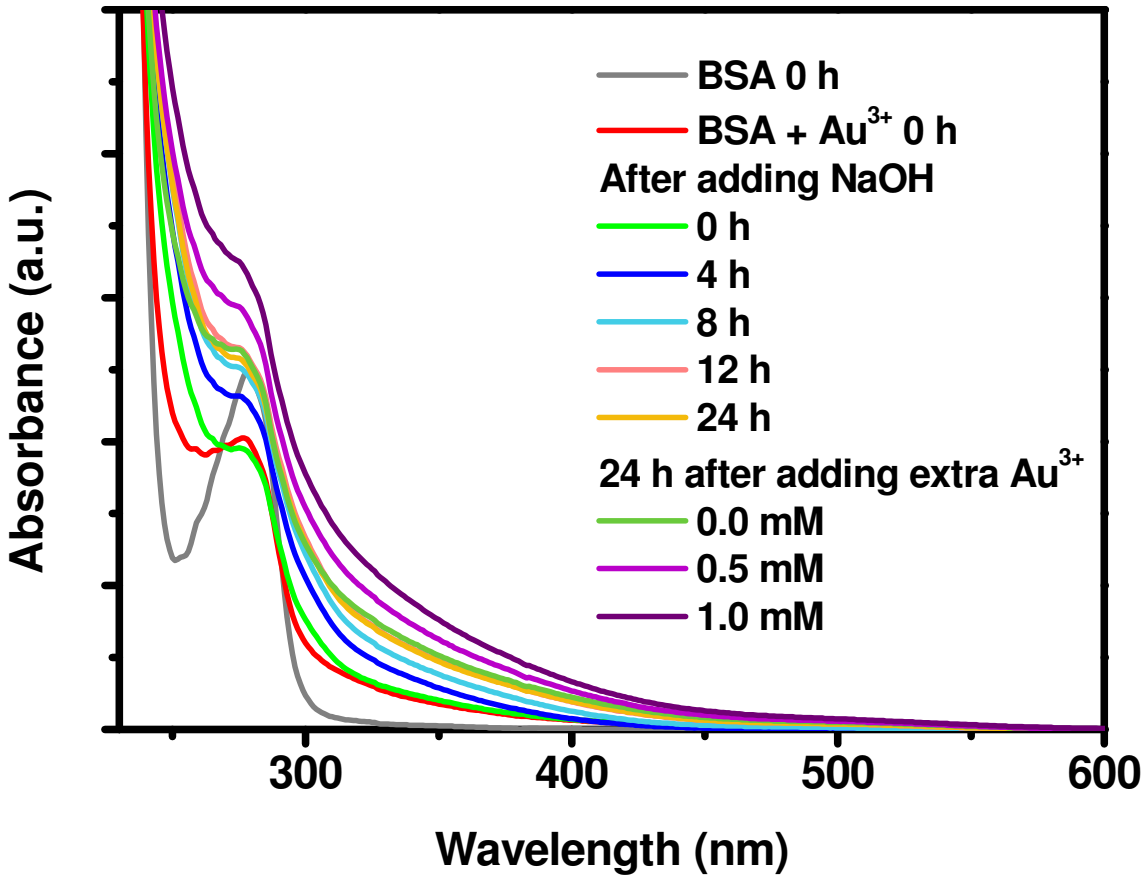

Figure S21. UV-Vis spectra of Au_{QC}@BSA at various stages of evolution.

Supporting information 22. PL spectra of Au_{QC}@BSA at various stages of evolution.

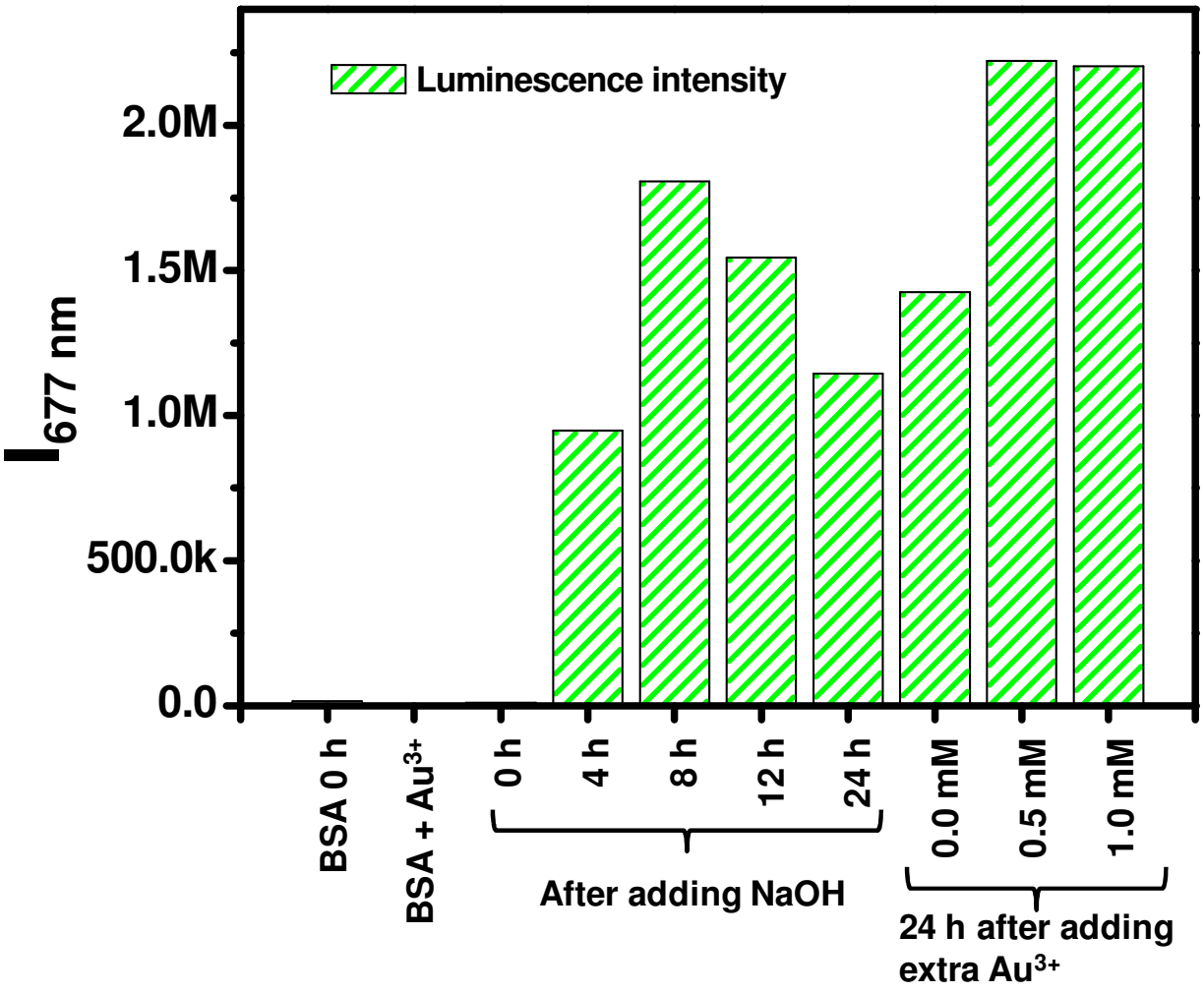

Figure S22. PL spectra of Au_{QC}@BSA at various stages of evolution. Average emission peak position was found to be 677 nm for Au_{QC}@BSA, hence PL intensity was compared at 677 nm. It can be seen that as emergence of parent protein takes place after 8 h, PL intensity decreases. Then after adding extra Au^{3+} to consume parent protein, increase in the PL intensity was observed.